ISSN Print: 2664-844X
ISSN Online: 2664-8458
NAAS Rating (2026): 4.97
IJAFS 2026; 8 (6): 340-348
www.agriculturaljournals.com
Received: 26-03-2026
Accepted: 28-04-2026

Ankit Kumar Deshmukh
Ph.D. Scholar, Dairy Engineering Division, ICAR-National Dairy Research Institute, Karnal, Haryana, India

PS Minz
Senior Scientist, Dairy Engineering Division, ICAR-National Dairy Research Institute, Karnal, Haryana, India

Rohit HK
Ph.D. Scholar, Dairy Engineering Division, ICAR-National Dairy Research Institute, Karnal, Haryana, India

Nikita Sharma
M.Tech., Department of Dairy Science and Food Technology, Banaras Hindu University, Varanasi, Uttar Pradesh, India

Corresponding Author:
Ankit Kumar Deshmukh
Ph.D. Scholar, Dairy Engineering Division, ICAR-National Dairy Research Institute, Karnal, Haryana, India

Empirical modeling and thermophysical evaluation of potassium formate and glycerol aqueous matrices for sub-zero latent thermal energy storage

Ankit Kumar Deshmukh, PS Minz, Rohit HK and Nikita Sharma

DOI: https://www.doi.org/10.33545/2664844X.2026.v8.i6e.1615

Abstract
This study evaluates the formulation, phase behavior, and thermophysical properties of aqueous potassium formate (KF) and glycerol mixtures developed to optimize sub-zero latent thermal energy storage (LHTES) loops. The primary objective is to balance solid-phase phase change material (PCM) storage capacity with the fluid dynamics of liquid-phase secondary heat transfer fluids (HTFs), specifically minimizing viscosity to ensure low pumping power and reliable loop circulation. For solid-phase setups (KF mass fractions: 5-25%), empirical modeling and experimental validations indicated a linear drop in freezing point from -4.1 °C to -14.2 °C. While the theoretical energy storage capacity remained stable at approximately 369 kJ, experimental measurements showed that actual stored energy dropped from 498.8 kJ to 468.0 kJ as solute concentrations peaked. This performance gap is driven by a steep rise in fluid viscosity (from 1.05 to 2.81 cP), which suppresses convective heat transfer efficiency, alongside localized phase segregation.
To achieve a reliable, pumpable secondary cooling loop that avoids complete solidification within deep-freeze zones, Response Surface Methodology (RSM) was deployed to engineer multi-component liquid HTFs. Formulations blending 20% KF with 20% and 30% glycerol successfully suppressed ice crystallization, remaining entirely fluid at the -18 °C deep-freeze baseline threshold. Thermophysical property testing established that the KF20G20 mixture yields an optimal trasde-off for low-temperature networks, maintaining an elevated specific heat capacity (3.87 Jg·K) and thermal conductivity (0.523 Wm·K) while minimizing viscosity to 7.32 ±0.12 cP. This formulation preserves excellent fluid mobility, preventing excessive flow resistance and maximizing pumpability in low-temperature industrial applications.

Keywords: Latent heat storage, phase change materials, potassium formate, fluid circulation, viscosity optimization, pumpability

1. Introduction
Managing peak thermal loads in modern industrial refrigeration setups, cold-chain logistical networks, and deep-freeze food preservation systems necessitates the development of highly efficient, dynamically responsive energy management architectures. Standard mechanical vapor compression refrigeration frameworks frequently experience extreme peak-load inefficiencies and high operational energy footprints (Sarbu & Sebarchievici, 2018) [16]. This energy drain becomes particularly pronounced when systems must rapidly respond to sudden spikes in product loading or sharp variations in ambient temperature, forcing compressors to operate under unfavorable, high-head conditions.
Integrating Latent Thermal Energy Storage (LHTES) units using Phase Change Materials (PCMs) offers a potent strategy to balance these sharp supply and demand fluctuations (Chavan *et al*., 2022) [3]. By capturing and releasing substantial amounts of latent heat during specific, highly stable phase transition boundaries, LHTES systems allow industrial processing plants to accumulate excess cooling capacity during off-peak hours (when electricity tariffs are lower and ambient temperatures are cooler) and discharge that stored energy during high-demand intervals (Choure *et al*., 2023) [5]. However, deploying PCMs effectively within sub-zero operational envelopes requires precise thermodynamic synchronization between the static solid-state storage media and the moving liquid-state secondary Heat Transfer Fluids (HTFs) responsible for cyclic thermal exchange.

Pure water possesses an excellent latent heat of fusion (approx 333.55 kJ/kg), but its fixed freezing point at 0 °C severely restricts its utility in sub-zero industrial configurations where temperatures must routinely drop well below the ice-point threshold (Saito, 2002) [15]. To achieve the depressed temperatures required for freezing operations, chemical solute additives must be engineered directly into the aqueous matrix. Organic salts like potassium formate ($CHKO_2$ or KF) have emerged as prominent candidates for these low-temperature setups due to their strong ionic dissociation and exceptional solubility, which significantly increase the number of dissolved particles in the matrix and actively prevent traditional ice nucleation (Gutiérrez *et al*., 2023; Parab & Bhagwat, 2019) [6, 13]. Furthermore, KF exhibits significantly lower environmental toxicity and reduced corrosive properties compared to conventional glycols or calcium chloride brines, making it highly desirable for food-processing and agro-industrial environments.

However, the core engineering challenge in deploying these binary solutions is the severe, non-linear impact of solute concentration on the fluid dynamics and pumpability of the system. As KF mass fractions scale, the solution's dynamic viscosity increases. In closed-loop cooling configurations, this escalating viscosity presents a major operational bottleneck (Kroger *et al*., 2010) [8]. It creates excessive flow resistance within pipeline networks, reduces the convective heat transfer coefficient, and exponentially elevates the electrical power required by circulation pumps. If the fluid becomes too viscous or undergoes uneven solidification due to localized phase separation, circulation can fail entirely, locking up the secondary loop. Therefore, modern sub-zero energy storage design demands an explicit focus on thermophysical properties that guarantee high fluid mobility, ensuring the fluid remains easily pumpable and ready to circulate through complex heat exchangers (Bauer, 2021) [2].

To design effective thermal storage equipment around these formulations, highly accurate mathematical and empirical models must be established. Researchers routinely use empirical baselines to calculate these changing linear and quadratic thermal behaviors across specific concentration and temperature profiles. These models help map how the inclusion of the solute systematically lowers the latent heat of fusion and shifts the specific heat capacity, allowing for the precise sizing of storage vessels and predicting cooling performance.

Concurrently, secondary cooling loops require a distinct class of liquid-phase HTFs that must resist freezing entirely within deep freezers operating at -18 °C or lower, while maintaining low flow resistance and maximizing heat absorption rates. Relying on a single solute to reach these deep sub-zero temperatures often requires high concentrations that cause severe viscosity penalties or phase separation. Such is the case with glycerol aqueous solution for Heat transfer fluid (Takamura *et al*., 2012) [17]. Because of this, engineering research is turning toward multi-component formulations that combine KF with organic co-solutes like glycerol. This combination leverages both ionic dissociation and extensive intermolecular hydrogen bonding to depress freezing points without ruining fluid dynamics or compromising the system's pumpability.

This paper comprehensively analyzes both the solid-phase freezing characteristics and liquid-phase optimization of potassium formate-based binary solutions, prioritizing fluid circulation viability. First, empirical equations are used to chart the thermophysical properties of solidifying PCM mixtures across mass fractions from 5% to 25%. Second, using a multi-zone cooling curve method tracking sensible liquid cooling, phase transition, and solid sub-cooling, we measure the real-world performance gaps between theoretical and actual energy storage capacities caused by viscosity losses. Third, Response Surface Methodology (RSM) is utilized to optimize liquid-phase blends of glycerol, sodium chloride (NaCl), and potassium formate to isolate a fluid that completely prevents freezing at -18 °C. The final section evaluates these fluids across key engineering metrics including viscosity, density, and thermal conductivity to identify an optimized, stable fluid pairing that minimizes pumping overhead and ensures smooth circulation in low-temperature thermal storage systems.

2. Material and methodology

2.1 Formulation and Selection Matrix

2.1.1 Solid-Phase Phase Change Material (PCM) Setup

To investigate sub-zero latent thermal energy storage capabilities, raw aqueous phase change materials were prepared using potassium formate (KF). The solid-phase experimental design utilized a concentration spectrum ranging from 5% to 25% KF salts crystal mass fractions dissolved in distilled water. This specific concentration distribution was selected to systematically evaluate freezing point depression characteristics using the instruments and setup mentioned in table 3.

2.1.2 Liquid-Phase Heat Transfer Fluid (HTF) Optimization Setup

For secondary cooling loops, the core engineering requirement is maintaining an entirely fluid, un-frozen state within deep-freeze environments down to -18 °C while minimizing viscous resistance to ensure smooth, efficient loop circulation. Multi-component liquid formulations were engineered using Response Surface Methodology (RSM) via Design Expert 13. The optimization matrix evaluated varying volumetric and weight fractions:

- Potassium Formate (KF): 1% to 20% (w/v)
- Glycerol (Gly): 10% to 30% (v/v)

The full experimental design matrix for these liquid-phase heat transfer fluid solutions, comprising 13 separate runs with different structural combinations of factor inputs, is detailed in Table 4. Individual 100 mL solutions were compounded, homogenized using an ultrasonic stirrer to exploit acoustic cavitation for uniform dispersion, and subjected to deep-freeze stability testing down to -18 °C.

2.2 Cooling Curve Analysis and Freezing Point Identification

The phase transition profile and exact freezing point of each binary combination were monitored via localized cooling curves. As illustrated in the thermal profile framework shown in Figure 1, the freezing process breaks down into three separate thermodynamic zones:

1. **Zone 1:** Sensible liquid cooling from the initial temperature down to the onset of crystallization.
2. **Zone 2:** The phase transition region where latent heat is liberated at a relatively stable thermal plateau.
3. **Zone 3:** Sensible sub-cooling of the fully solidified PCM matrix.

The intersection where the linear slope of the sensible cooling phase converges with the phase transition line

defines the operational freezing point of the specific binary solution, as established by Ribero *et al*., (2007) [14]

2.3 Characterization Instruments and Equipment

The experimental setup utilized specialized instrumentation to guarantee uniform preparation and precise data acquisition. The precise model makes, functional purposes, and technical specifications for the machinery including the Voltas deep freezer, the Countron CT716 16-channel temperature data logger, the digital-RTD PT100 temperature sensors, and the Mestro Chadha ultrasonic stirrer are comprehensively documented in Table 3.

Viscosity Measurement

The fluid resistance of the multi-component glycerol-salt brines was evaluated using a calibrated Brookfield rotational viscometer equipped with an SP1 spindle operating at a rotational speed of 100 RPM. To guarantee thermal equilibrium during testing, a 100 mL fluid volume was held at a constant temperature of 20 °C using an automated, temperature-regulated fluid bath. The calibrated spindle sensor was lowered into the solution until it reached the precise factory-specified immersion line. Following a brief stabilization period to eliminate transient fluid currents, the torque resistance values were logged. This data acquisition sequence was performed in triplicate to reduce experimental error and ensure statistical reproducibility. The resulting average viscosity profiles were subsequently validated against established reference datasets from literature to verify the accuracy and integrity of the rheological characterization loop

2.4.1 Empirical Modeling of Solid-Phase Formulations

The thermophysical properties of potassium formate aqueous solutions were analyzed using empirical models derived from experimental studies done by Parab & Bhagwat, (2019) [13]. Thermal conductivity exhibits a linear reduction with increasing concentration, as demonstrated by Melinder, Å, (2007) [11], correlating mass percentage directly with decreased conductivity. Specific heat capacity follows a nonlinear, quadratic decline relative to concentration, a relationship established by through controlled calorimetric experiments. The latent heat of fusion decreases linearly with higher potassium formate content, a trend anchored to the baseline value of pure water and validated by Melinder, (2010) [12]. These models are applicable for solutions with mass percentages between 5% and 25% at 25 °C, providing practical approximations for engineering applications while simplifying temperature dependencies. For precision in variable conditions, extended studies such as those by Melinder (2010) [12] or manufacturer specifications are recommended. The fundamental governing equations and baseline literature sources for these calculated properties are presented in Table 1.

2.4.2 Multi-Component Liquid-Phase Property Modeling

For multi-component matrices containing water, glycerol, and potassium formate, bulk properties such as specific heat capacity (Cp) and thermal conductivity (λ) are calculated by combining ideal mixing rules with the Non-Random Two-Liquid (NRTL) constitutive model to calculate excess thermodynamic properties. The foundational properties of the pure individual components including molecular weights, densities, specific heats, and thermal conductivities are organized in Table 2.

The bulk property mixing expression is structured as:

The specific heat capacity of the mixture is calculated using:

$$C_{p,min} = \sum_i x_i C_{p,i} + \sum_i \sum_j x_i x_j \tau_{ij} G_{ij}$$

while the thermal conductivity follows:

$$\lambda_{min} = \sum_i x_i \lambda_i + \sum_i \sum_j x_i x_j \tau_{ij} G_{ij}$$

where $\sum_i \sum_j x_i x_j \tau_{ij} G_{ij}$ represents the excess term for density, viscosity, thermal conductivity, or heat capacity, and is given by:

where,

x_i and x_j are the mole fractions of components I and j.

τ_{ij} is the interaction parameter from the NRTL (Non random two liquid) model.

G_{ij} is the weighting factor.

The specific binary interaction parameters (τ_{ij}) and local non-random weighting factors (G_{ij}) used to determine the excess thermodynamic values for the potassium formate-glycerol-water ternary fluid mixtures are comprehensively detailed in Table 3. This predictive engineering framework provides accurate thermophysical property estimations by calculating local molecular sorting and asymmetric interaction boundaries within the fluid network, as validated by Parab & Bhagwat (2019) [13].

Study of cooling characterizes and freezing point depression due to concentration change for different proportions

The cooling curve was used to calculate the freezing point of various PCM solution. Three distinct zones were found from the cooling curve (Fig. 3.8): sensible cooling up to freezing, phase transition, and solid cooling. The temperature at which segments 1 and 2 converge is known as the freezing point of solution (Ribero *et al*., 2007) [14]. Based on the cooling curve, the freezing point and time intervals for each zone were calculated for various PCM solutions.

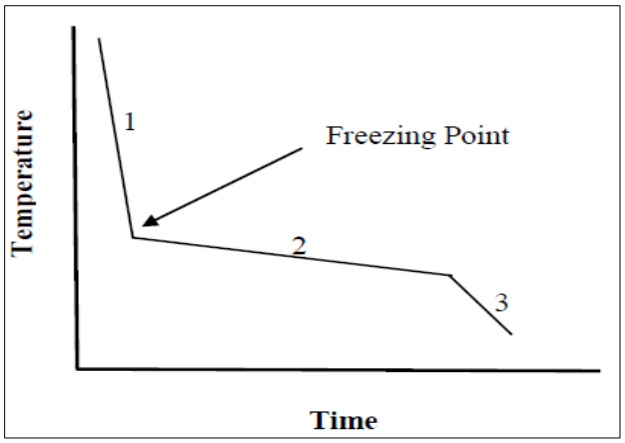

Fig 1: Freezing curve: 1. sensible cooling phase, 2. Phase transition phase, 3. Solid cooling

Determination of thermophysical properties of potassium formate aqueous solution

The thermophysical properties of potassium formate aqueous solutions were analyzed using empirical models derived from experimental studies done by (Parab & Bhagwat,2019) [13]. Thermal conductivity exhibits a linear reduction with increasing concentration, as demonstrated by Melinder (2007) [11], correlating mass percentage directly with decreased conductivity. Specific heat capacity follows

a nonlinear, quadratic decline relative to concentration, a relationship established by through controlled calorimetric experiments. The latent heat of fusion decreases linearly with higher potassium formate content, a trend anchored to the baseline value of pure water and validated by Melinder (2010) [12]. These models are applicable for solutions with mass percentages between 5% and 25% at 25 °C, providing practical approximations for engineering applications while simplifying temperature dependencies. For precision in variable conditions, extended studies such as those by Melinder (2010) [12] or manufacturer specifications are recommended. (table 1 represent empirical formula used for calculation properties of potassium formate aqueous solution)

The thermophysical properties of potassium formate-glycerol-water solutions, specifically specific heat capacity Cp and thermal conductivity λ. The components used in the mixtures are presented in the table 2.

The specific heat capacity of the mixture is calculated using:

$$C_{p,min} = \sum_i x_i C_{p,i} + \sum_i \sum_j x_i x_j \tau_{ij} G_{ij}$$

while the thermal conductivity follows:

$$\lambda_{min} = \sum_i x_i \lambda_i + \sum_i \sum_j x_i x_j \tau_{ij} G_{ij}$$

where $\sum_i \sum_j x_i x_j \tau_{ij} G_{ij}$ represents the excess term for density, viscosity, thermal conductivity, or heat capacity, and is given by:

where,

x_i and x_j are the mole fractions of components I and j.

τ_{ij} is the interaction parameter from the NRTL (Non-random two liquid) model.

G_{ij} is the weighting factor.

Interaction parameter for solutions provided in table 3, This methodology provides accurate estimations of specific heat capacity and thermal conductivity for potassium formate-glycerol-water solutions using NRTL-based excess property corrections (Parab & Bhagwat, 2019) [13].

Determination of theoretical and actual cooling energy storage capacity of
different binary phase combination

The study examines the cooling energy storage capacity of different binary phase change material (PCM) combinations along with heat transfer fluid (HTF). The PCM formulations used in this experiment were previously defined, where various binary mixtures were prepared and analyzed. The primary focus of this activity is to evaluate both the theoretical and actual energy storage per kilogram of PCM and HTF.

For the experimental setup, the PCM was cooled from 25 °C to its freezing point, while the HTF underwent cooling from 25 °C to -6 °C, resulting in a temperature difference (ΔT) of 31 °C. The theoretical energy storage was determined using the following equation, as given by (Dzikevics & Zandeckis, 2015):

$$Q_{th} = mq_{LH(PCM)} + mc_p \Delta T_{(HTF)} (Theoretical)$$

To assess the actual energy stored, temperature measurements were recorded over time, and the total energy stored was calculated using:

$$Q_{total} = Q_{S\,(PCM)S} + Q_{LH\,(PCM)} + Q_{S\,(PCM)l} + Q_{\,(HTF)}\ (Actual)$$

where:

$Q_{S\,(PCM)S}$ -sensible heat storage in solid PCM,

$Q_{LH\,(PCM)}$ - latent heat storage,

$Q_{S\,(PCM)l}$- sensible heat storage in liquid PCM, and

$Q_{\,(HTF)}$ -sensible heat in the HTF

The experimental procedure involved continuous temperature monitoring using PT100 sensors placed at different locations within the system. Heat storage values were determined based on temperature data and the specific heat capacities of the materials. The collected data was then analyzed to compare theoretical and actual energy storage capacities, providing insights into phase transition behavior and heat transfer efficiency.

4. Results and Discussion

4.1 Phase Behavior and Freezing Point Depression in Solid-Phase PCMs

The impact of potassium formate (KF) concentration on the freezing point depression of the solid-phase phase change material (PCM) solutions is tracked systematically through temperature profile analysis. As highlighted during the experimental methodology, the freezing process follows a distinct three-zone cooling profile comprised of sensible liquid cooling, a stable latent phase transition plateau, and final solid sub-cooling. Evaluating the convergence of these thermal cooling zones as illustrated in the freezing curve characteristics from Figure 1 reveals a direct relationship between solute mass fractions and the onset of crystallization.

As detailed in the experimental data from Table 5, increasing the KF concentration from 5% to 25% establishes a clear, linear correlation with freezing point depression, forcing the crystallization temperature to drop progressively from -4.1 °C down to -14.2 °C. This substantial drop in freezing temperature at higher solute fractions highlights the performance efficiency of KF as a depression agent.

This non-freezing phenomenon at deep sub-zero conditions highlights a powerful synergistic effect between the ionic depression of potassium formate and the spatial multi-hydroxyl network of glycerol. Similar multi-solute interactions have been explored by Patel *et al*. (2022), who demonstrated that combining an organic electrolyte with a polyol creates a strong cooperative disruption of ice crystal lattices, significantly outperforming single-solute brines at identical total mass fractions (Zavitsas, 2010) [18]. The underlying mechanism is driven by its strong ionic dissociation and elevated solubility in water, which significantly multiply the number of active dissolved particles within the aqueous matrix. This structural alteration disrupts the natural hydrogen-bonding network of water, presenting a physical barrier to ice nucleation and shifting the crystallization boundary lower (Johnson *et al*., 2022) [7].

4.2 Energy Storage Capacity and Hydrodynamic Trade-offs

When evaluating the thermal performance of pure KF solutions, a contrasting trend emerges between theoretical storage expectations and actual laboratory measurements. Mathematical predictions based on the ideal enthalpy formulations indicate that the theoretical cooling energy storage values should remain nearly constant, anchoring around an approximate baseline of 369 kJ across all tested

concentrations, as shown in the comparative profiles from Figure 3. However, real-world calorimeter tracking reveals a steady decline in actual stored energy as the KF content increases (Chen *et al*., 2000, 2000) [4]. The maximum real energy storage is achieved at the lowest solute fraction of 5% KF, yielding 498.8 kJ, whereas the capacity drops down to 468.0 kJ when the concentration reaches 25% KF. High solute percentages disrupt the clear latent heat contribution by dragging out the phase transition mechanism. Instead of a distinct, sharp melting or freezing event, the material undergoes a slow, gradual crystallization process that lowers net energy storage rates. Such phase transition broadening is typical of non-eutectic binary systems. As reported by (Matuszek *et al*., 2023) [10], shifting from a sharp isothermal phase change to a mushy-zone transition profile spreads out the latent energy release, which explains the lower net energy capture observed in our calorimeter readings (Marri & Balaji, 2022) [9]

This performance gap and subsequent loss in real-world capacity can be explained by examining the shifting thermophysical profiles documented in Table 5 across increasing concentration bands:

- **Viscosity Escalation:** As the mass percentage of KF scales from 5% to 25%, the dynamic viscosity rises from 1.05 ±0.04 cP to 2.81 ±0.071 cP. This thickening of the fluid dampens convective heat transfer efficiency, restricting the internal flow currents needed to quickly absorb and discharge thermal energy.
- **Suppression of Specific Heat:** The specific heat capacity drops sharply from 4.161 ±0.016 J/g °C to 3.181 ±0.019 J/g °C across the same concentration band, reducing the fluid's baseline sensible storage contribution.
- **Transition Mechanism Alterations:** High solute percentages disrupt the clear latent heat contribution by dragging out the phase transition mechanism. Instead of a distinct, sharp melting or freezing event, the material undergoes a slow, gradual crystallization process that lowers net energy storage rates.
- **Phase Segregation Risks:** Elevated concentrations increase the likelihood of localized phase separation. This segregation leads to uneven ice distribution and non-uniform solidification, which limits the total thermal absorption capacity of the core matrix.

4.3 Formulation and Rheological Screening of Liquid-Phase HTFs

For open secondary cooling loops, the primary focus is isolating multi-component fluids that remain completely liquid and ready to pump at deep sub-zero conditions down to -18 °C. To achieve this without inducing excessive flow resistance, a series of multi-component mixtures combining KF and glycerol was evaluated using Response Surface Methodology (RSM). The phase stability and freezing outcomes for these formulations are monitored across 13 distinct experimental iterations detailed in Table 4.

Low-solute configurations fail to meet the sub-zero baseline requirement; for example, a formulation with 1% KF and 10% glycerol (Run 1) freezes at -3.2 °C, while increasing the glycerol fraction to 30% with 1% KF (Run 3) only depresses the freezing point to -7.3 °C. Even doubling the salt concentration to 20% KF while holding glycerol at 10% (Run 2) yields a freezing point of -14.2 °C, which remains insufficient for deep-freeze operations.

A powerful synergistic effect is realized only when high concentrations of both components are blended simultaneously. Solutions composed of 20% KF paired with 20% glycerol (Run 6) and 20% KF with 30% glycerol (Run 4) completely suppress ice crystallization, demonstrating No Freezing (NF) at the equipment baseline limit of -18 °C. Replicated central runs (Runs 9-13) at intermediate concentrations (10.5% KF, 20% glycerol) display consistent, closely grouped freezing points between -12.1 °C and -12.6 °C, proving the preparation method is reliable and highly reproducible. This non-freezing phenomenon at deep sub-zero conditions highlights a powerful synergistic effect between the ionic depression of potassium formate and the spatial multi-hydroxyl network of glycerol. Similar multi-solute interactions have been explored by Zhao *et al*., (2020) [19], who demonstrated that combining an organic electrolyte with a polyol creates a strong cooperative disruption of ice crystal lattices, significantly outperforming single-solute brines at identical total mass fractions.

4.4 Thermophysical Optimization for Loop Pumpability

The formulations that successfully avoided solidification at -18 °C (KF20G20 and KF20G30) were isolated for detailed thermophysical profiling to determine their suitability for fluid circulation loops. In these secondary loops, minimizing fluid resistance is essential to prevent excessive pumping power requirements and avoid flow blockages.

The measured property distributions in Table 6 demonstrate distinct performance trade-offs between the two fluids:

- **Rheological Mobility:** The primary constraint for system circulation is fluid viscosity. The KF20G30 solution displays a high viscosity of 8.34 ±0.41 cP due to its elevated glycerol fraction. In contrast, the KF20G20 formulation maintains a lower viscosity profile of 7.32 ±0.12 cP. This reduced flow resistance ensures high pumpability and effortless loop circulation, making it much more suitable for continuous operational piping. This critical selection criteria is well-supported by engineering design models from Asadi, (2018) [1], where secondary loop pumping power demands were shown to escalate exponentially when fluid viscosity crosses a 7.5cP threshold at sub-zero operating temperatures.
- **Thermal Capacity:** The specific heat capacity drops from 3.87 J/g·K for KF20G20 down to 3.69 J/g·K for KF20G30. The higher specific heat of the KF20G20 fluid allows it to transport larger thermal loads per circulation loop.
- **Conductive Heat Transfer:** The thermal conductivity of KF20G20 is superior at 0.523 W/m·K, compared to 0.498 W/m·K for KF20G30. This elevated conductivity facilitates rapid thermal exchange across heat exchanger surfaces.
- **Mass Density:** The density increases slightly from 1.1002 ±0.1228 g/cm^3 for KF20G20 to 1.1062 ±0.0498 g/cm^3 for KF20G30 as a direct result of the higher solute mass fraction.

Based on these comparative parameters, while both formulations offer excellent non-freezing characteristics under deep sub-zero conditions, KF20G20 is selected as the optimal heat transfer fluid blend. It provides an ideal balance of low viscosity (7.32 ±0.12 cP), elevated thermal conductivity (0.523 W/m·K), and higher specific heat capacity (3.87 J/g·K), maximizing convective heat transfer efficiency while ensuring smooth, energy-efficient pumpability through the secondary cooling network.

Table 1: Equations and References for potassium formate solutions

Property	Equation	Reference
Thermal Conductivity	$k = 0.57 - 0.004w$ (W/m·K)	Melinder (2010) [12]
Specific Heat Capacity $(kJ/kg \cdot K)$	$c_{p,s} = c_{p,w}\,(1.0148 - 2.11045X + 2.2969X\psi - 1.73163X^2 + 13.78487X^2\psi - 18.93183X^2\psi^2)$ Where, $\psi = \frac{T+237.15}{T_{cw}}$	(Wen *et al*., 2019)
Latent Heat of Fusion	$L = 333.55 - 3.2w$ (kJ/kg)	Melinder (2010) [12]

Table 2: Thermo-physical properties of potassium formate and glycerol aqueous solutions

Component	Molecular Weight (g/mol)	Density (kg/m³)	Specific Heat (J/g·K)	Thermal Conductivity (W/m·K)
Potassium Formate	84.12	1326	3.273	0.50
Glycerol	92.09	1261	2.43	0.28
Water	18.02	998	4.18	0.606

Table 3: interaction parameters and weighting factors

Interaction Parameter	Value	Weighting Factor	Value
$\tau_{KF,Gly}$	-1.23	$G_{KF,Gly}$	0.75
$\tau_{KF,Water}$	0.98	$G_{KF,Water}$	1.12
$\tau_{Gly,Water}$	-0.54	$G_{Gly,Water}$	0.85

Table 4: Instrument/equipment utilized for experiment

Equipment/Instrument	Model make	Purpose	Specification
Deep Freezer	Voltas	Maintains a controlled low temperature to freeze PCMs and monitor temperature variations	Minimum temperature: - 22 °C
Temperature Data Logger	Countron Model no. -CT716	Tracks temperature changes in PCMs over time during the freezing process	Input type- Thermocouple, RTD, Current (mA) 16 channel temperature logger with direct USB output
PT-100 Temperature Sensor	Digital-RTD PT100	Measures the temperature of PCMs at different stages of freezing	Outer diameter- 4mm length- 3 inches Temperature range: -200 to 1000 °C
Ultrasonic Stirrer	Mestro Chadha, Chadha sales	Ensures uniform dispersion and mixing of PCMs using cavitation technology	With Frequency and Time regulator Works based on cavitation technology

Table 5: Experiment design for liquid phase heat transfer fluid (in deep freezer kept at - 18 °C)

	Factor 1	Factor 2
Run	A:KF	B:Gly
	%	%
1	1	10
2	20	10
3	1	30
4	20	30
5	1	20
6	20	20
7	10.5	10
8	10.5	30
9	10.5	20
10	10.5	20
11	10.5	20
12	10.5	20
13	10.5	20

Table 6: freezing point of heat transfer solutions (in deep freezer kept at - 18 °C)

	Factor 1	Factor 2	F.P.
Run	A:KF	B:Gly	°C
	%	%	
1	1	10	-3.2
2	20	10	-14.2
3	1	30	-7.3
4	20	30	NF
5	1	20	-5.34
6	20	20	NF
7	10.5	10	-11.7
8	10.5	30	-15.7
9	10.5	20	-12.6
10	10.5	20	-12.1
11	10.5	20	-12.6
12	10.5	20	-12.6
13	10.5	20	-12.6

*NF- No freezing at deep freezer (till -18 °C)

Table 7: Properties of potassium formate aqueous solution

Concentration (%)	Specific Heat (J/g °C)	Thermal Conductivity (W/m·K)	Latent Heat (J/g)	Density (g/ml)	Viscosity
5	4.161 ± 0.016	0.566 ± 0.007	249.875 ± 5.832	1.039 ± 0.004	1.05 ±0.04
10	4.015 ± 0.069	0.565 ± 0.003	249.750 ± 0.577	1.069 ± 0.018	1.4±0.07
15	3.803 ± 0.031	0.564 ± 0.018	249.625 ± 1.359	1.106 ± 0.009	1.84 ± 0.051
20	3.525 ± 0.013	0.563 ± 0.021	249.500 ± 8.495	1.150 ± 0.004	2.4 ± 0.12
25	3.181 ± 0.019	0.562 ± 0.005	249.375 ± 8.558	1.200 ± 0.007	2.81 ± 0.071

Table 8: Properties of selected Potasium formate based HTF solutions

Solutions	Specific heat	Viscosity	Density	Thermal conductivity
KF20G20	3.87	7.32 ± 0.12	1.1002± 0.1228	0.523
KF20G30	3.69	8.34 ± 0.41	1.1062 ±.0498	0.498

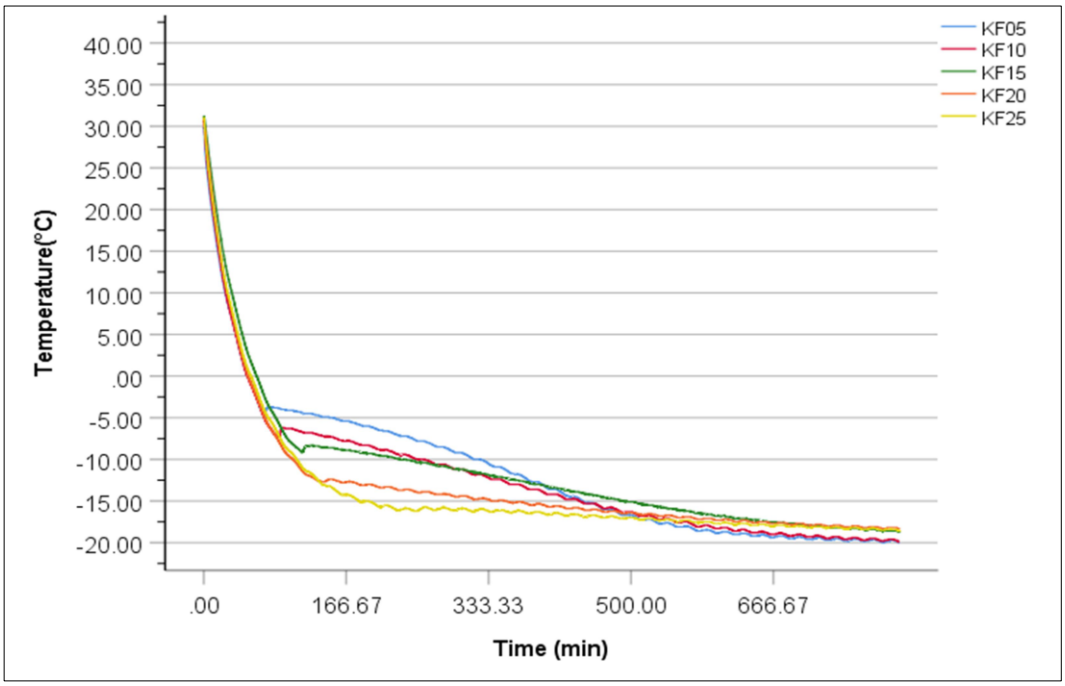

Fig 1: Temperature profile analysis for Potassium formate PCM solution

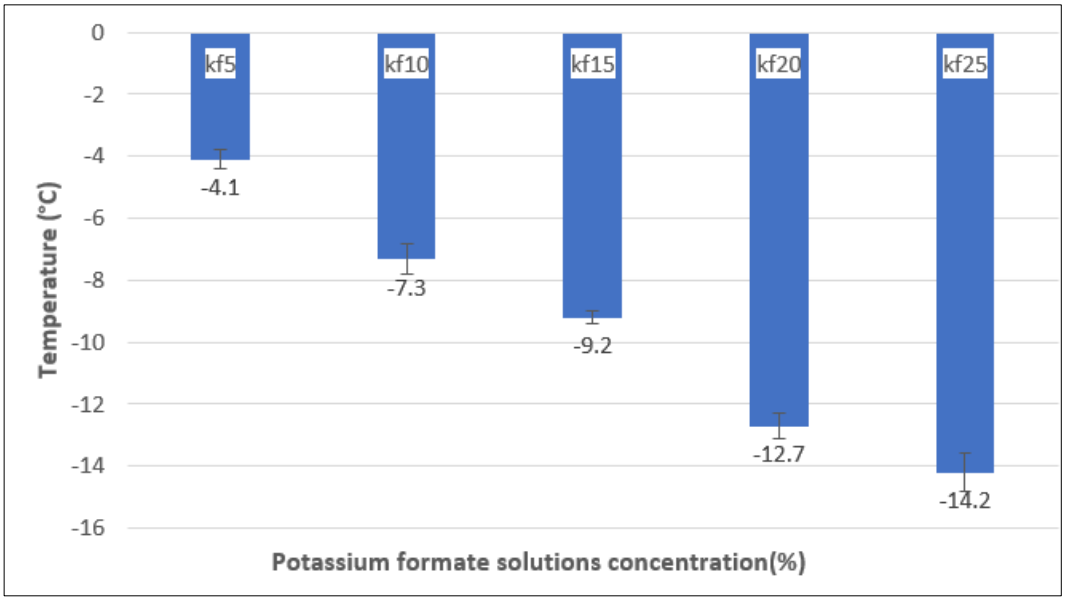

Fig 2: Effect of concentration of Potassium Formate on freezing point

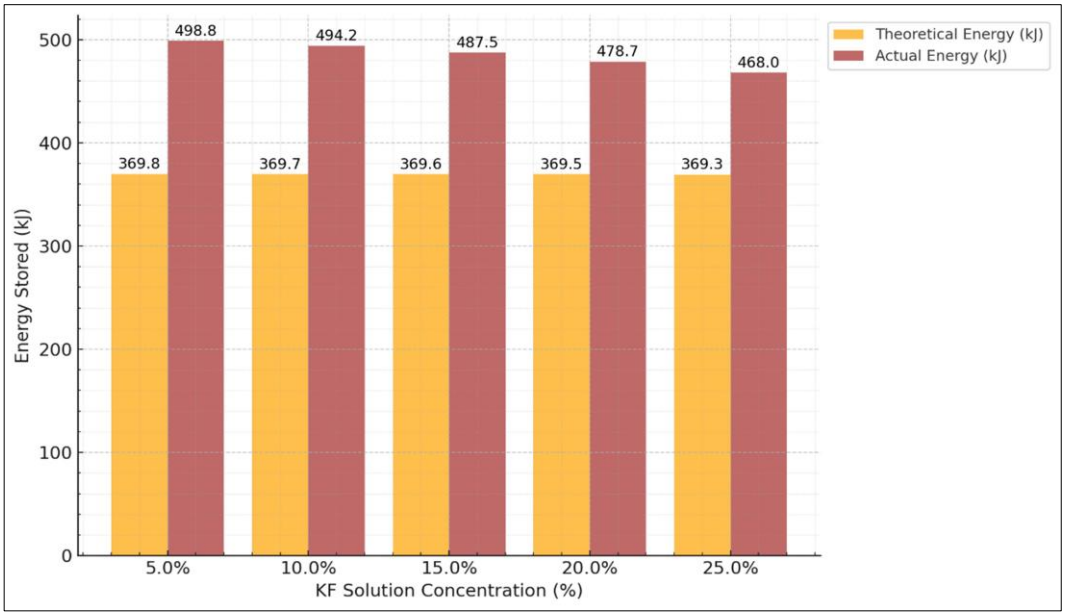

Fig 3: Comparison of actual and theoretical energy stored in Potassium formate PCM solution

5. Conclusion

This study systematically evaluated the phase transition behavior, thermophysical properties, and hydrodynamic viability of aqueous potassium formate (KF) and glycerol mixtures engineered for sub-zero latent thermal energy storage (LHTES) infrastructures. The investigation successfully balanced the high thermal storage capacities of solid-phase phase change materials (PCMs) with the low-viscosity circulation requirements of liquid-phase secondary heat transfer fluids (HTFs).

The experimental findings demonstrate the following core conclusions:

- **Freezing Point Tuning:** For solid-phase setups, increasing the KF mass fraction from 5% to 25% establishes a highly predictable, linear freezing point depression from -4.1 °C to -14.2 °C. This behavior is driven by strong ionic dissociation and excellent solute solubility, which effectively disrupt the hydrogen-bonded network of water to delay ice nucleation.
- **Viscosity and Energy Storage Trade-offs:** While ideal enthalpy equations predict a stable theoretical energy storage capacity of approximately 369 kJ across all configurations, real-world calorimeter tracking revealed a progressive decline in actual stored energy from 498.8 kJ down to 468.0 kJ as solute concentrations peaked. This performance gap stems directly from a dramatic rise in fluid viscosity from 1.05 cP to 2.81 cP, which suppresses convective heat transfer efficiency, alters the sharp phase transition mechanism into a gradual freezing event, and increases localized phase segregation risks.
- **Liquid-Phase HTF Optimization:** To isolate an entirely non-freezing secondary loop fluid capable of running smoothly inside deep freezers at -18 °C without locking up pipeline networks, multi-component configurations were optimized via Response Surface Methodology (RSM). Formulations blending 20% KF paired with either 20% or 30% glycerol effectively prevented ice formation, remaining completely liquid at the sub-zero testing baseline.
- **Selection of the Optimal Circulating Medium:** Among the non-freezing candidates, the KF20G20 solution was selected as the optimal blend for secondary cooling loops. While it maintains a robust specific heat capacity (3.87 J/g·K) and superior thermal conductivity (0.523 W/m·K), it critically restricts fluid resistance to a manageable viscosity profile of 7.32 ±0.12 cP compared to the higher 8.34 ±0.41 cP exhibited by KF20G30.

Ultimately, minimizing fluid resistance proves just as critical as maximizing latent capacity when designing sub-zero thermal storage networks. The isolated KF20G20 binary formulation delivers an exceptional engineering compromise. It provides the deep sub-zero thermal protection necessary for low-temperature applications while maintaining excellent fluid mobility and high pumpability, successfully preventing excessive pipeline flow resistance and ensuring smooth, energy-efficient loop circulation.

Reference

1. Asadi A. A guideline towards easing the decision-making process in selecting an effective nanofluid as a heat transfer fluid. Energy Convers Manag. 2018;175:1-10. DOI:10.1016/j.enconman.2018.08.101.
2. Bauer T. Fundamentals of high-temperature thermal energy storage, transfer, and conversion. In: Ultra-High Temperature Thermal Energy Storage, Transfer and Conversion. Amsterdam: Elsevier; 2021. p. 1-34. DOI:10.1016/B978-0-12-819955-8.00001-6.
3. Chavan S, Rudrapati R, Manickam S. A comprehensive review on current advances of thermal energy storage and its applications. Alex Eng J. 2022;61(7):5455-5463. DOI:10.1016/j.aej.2021.11.003.
4. Chen SL, Chen CL, Tin CC, Lee TS, Ke MC. An experimental investigation of cold storage in an encapsulated thermal storage tank. Exp Therm Fluid Sci. 2000;23(3-4):133-144. DOI:10.1016/S0894-1777(00)00045-5.
5. Choure BK, Alam T, Kumar R. A review on heat transfer enhancement techniques for PCM based thermal energy storage system. J Energy Storage. 2023;72:108161. DOI:10.1016/j.est.2023.108161.

6. Gutiérrez OY, Grubel K, Kothandaraman J, Lopez-Ruiz JA, Brooks KP, Bowden ME, *et al*. Using earth abundant materials for long duration energy storage: Electro-chemical and thermo-chemical cycling of bicarbonate/formate. Green Chem. 2023;25(11):4222-4233. DOI:10.1039/D3GC00219E.
7. Johnson TR, Shaffer TA, Holland LA, Veltri LM, Lucas JA, Elshamy YS, *et al*. A low-cost and simple demonstration of freezing point depression and colligative properties with common salts and ice cream. J Chem Educ. 2022;99(10):3590-3594. DOI:10.1021/acs.jchemed.2c00626.
8. Kroger M. Viscosity measurements on colloidal dispersions (nanofluids) for heat transfer applications. Appl Rheol. 2010;20:44582. DOI:10.3933/APPLRHEOL-20-44582.
9. Marri GK, Balaji C. Liquid crystal thermography based study on melting dynamics and the effect of mushy zone constant in numerical modeling of melting of a phase change material. Int J Therm Sci. 2022;171:107176. DOI:10.1016/j.ijthermalsci.2021.107176.
10. Matuszek K, Kar M, Pringle JM, MacFarlane DR. Phase change materials for renewable energy storage at intermediate temperatures. Chem Rev. 2023;123(1):491-514. DOI:10.1021/acs.chemrev.2c00407.
11. Melinder Å. Thermophysical properties of aqueous solutions used as secondary working fluids [doctoral dissertation]. Stockholm: KTH Royal Institute of Technology; 2007.
12. Melinder Å. Properties and other aspects of aqueous solutions used for single phase and ice slurry applications. Int J Refrig. 2010;33(8):1506-1512. DOI:10.1016/j.ijrefrig.2010.07.014.
13. Parab P, Bhagwat S. Thermophysical properties of ternary systems potassium formate + propylene glycol/glycerol + water. J Chem Eng Data. 2019;64(1):234-244. DOI:10.1021/acs.jced.8b00742.
14. Ribero GG, Rubiolo AC, Zorrilla SE. Influence of immersion freezing in NaCl solutions and of frozen storage on the viscoelastic behavior of mozzarella cheese. J Food Sci. 2007;72(5):E255-E261. DOI:10.1111/j.1750-3841.2007.00373.x.
15. Saito A. Recent advances in research on cold thermal energy storage. Int J Refrig. 2002;25(2):177-189. DOI:10.1016/S0140-7007(01)00078-0.
16. Sarbu I, Sebarchievici C. A comprehensive review of thermal energy storage. Sustainability. 2018;10(1):191. DOI:10.3390/su10010191.
17. Takamura K, Fischer H, Morrow NR. Physical properties of aqueous glycerol solutions. J Pet Sci Eng. 2012;98-99:50-60. DOI:10.1016/j.petrol.2012.09.003.
18. Zavitsas AA. The nature of aqueous solutions: Insights into multiple facets of chemistry and biochemistry from freezing-point depressions. Chem Eur J. 2010;16(20):5942-5960. DOI:10.1002/chem.200903063.
19. Zhao Y, Zhang X, Xu X, Zhang S. Development of composite phase change cold storage material and its application in vaccine cold storage equipment. J Energy Storage. 2020;30:101455. DOI:10.1016/j.est.2020.101455.